Coupling the epithelial-to-mesenchymal transition and metabolic reprogramming

Madeline Galbraith, Dongya Jia, Herbert Levine, and José Onuchic

Introduction

The hallmarks of cancer have been investigated for many years with focus typically on a single facet. One such hallmark is metastasis which remains a leading cause of cancer related deaths[1]. During the epithelial-to-mesenchymal transition (EMT) the cells progressively lose their cellular adhesion and apical-basal polarity, increasing a cell's capacity for migration, invasiveness, and resistance to apoptosis [2,3]. The EMT has consistently been implicated in cells acquiring metastatic potential[4,5] and may also play a role in therapeutic resistance [6]. Recently, a transition state, called a partial-EMT or hybrid E/M state, was hypothesized to combine the motility and invasiveness of the mesenchymal cells with the cellular adhesion seen in epithelial cells allowing for collective migration during metastasis [7–10]. The hybrid E/M state has since been experimentally verified in many cell lines and has been associated with therapy resistance alongside poor survival rates [11–13]. Fully understanding the behavior of the hybrid E/M phenotype, especially connected with other hallmarks of cancer, is still an active area of research.

Metabolic reprogramming is another hallmark of cancer in which tumor cells alter their metabolism based on environmental signals[1,14]. Cells typically utilize oxidative phosphorylation (OXPHOS) under normoxic conditions and glycolysis when there is a lack of oxygen. However, cancer cells prefer glycolysis even when oxygen is available, referred to as the Warburg effect [15,16]. During metastasis, cancer cells must be able to survive in multiple different environments resulting in these cells switching between different types of metabolism[17–20]. Metabolic reprogramming, specifically in the context of switching between

the OXPHOS and Warburg metabolic phenotypes, can lead to hybrid states[21–23] including a low-low phenotype associated with therapy resistance [24]. The hybrid OXPHOS and glycolysis metabolic phenotype has experimentally been seen to correspond to circulating tumor cells (CTCs) originating from breast cancer suggesting this phenotype is correlated with metastasis[25]. The high metastatic potential of cancer cells with a hybrid metabolic phenotype was confirmed with additional experiments [26,27].

It has become increasingly clear that the crosstalk between EMT and metabolic reprogramming is important to metastasis and tumor proliferation [27–30]. Recent studies continue to confirm this interplay where metabolic reprogramming can increase metastatic potential and drive EMT, or EMT can drive metabolic reprogramming [31–34]. The exact mechanism of interaction between EMT and metabolic reprogramming is still unknown, Kang et al have suggested cancer cells undergo metabolic reprogramming before completing EMT and lastly becoming metastatic [35]. Given the distinct metabolic needs as cells complete EMT, another hypothesis is the mutual activation of EMT and metabolic reprogramming such that the transition states (hybrid E/M and hybrid glycolysis/OXPHOS) become coupled leading to a greatly increased metastatic potential[27]. Recently, high levels of both OXPHOS and glycolysis were noticed in CTCs [25] which have been shown to mainly consist of hybrid E/M cells if OXPHOS is upregulated [36]. Consistent results are seen when comparing mesenchymal breast cancer stem cells (M-BCSCs) to E/M-BCSCs, the E/M-BCSCs have high levels of OXPHOS and glycolysis as compared to M-BCSCs [37,38]. While there have been preliminary indications of the role EMT and metabolic reprogramming crosstalks play in metastasis and tumor proliferation, there is still much to be explored.

To decode the coupled decision-making of EMT and metabolism, we coupled the core gene regulatory circuits of EMT [7] and metabolic reprogramming [22] to elucidate the coupling of phenotypes and propose a mechanism of the interplay. We found that ROS is a key upregulator of the hybrid E/M state coupled with hybrid glycolysis/OXPHOS metabolic phenotype (hybrid E/M-W/O state) while Hif-1 may have slightly stronger affects than AMPK on the EMT network. When crosstalks between the circuits are active in both directions (EMT regulating metabolism, and vice versa), there are regions in which the hybrid E/M-W/O state was the only accessible state. Interestingly, if the system was modified to exclude the hybrid states when the crosstalks are inactive (i.e., neither the E/M or W/O states are initially accessible), once active, the crosstalks are able to modulate the phase space to generate the hybrid states. In fact, a single crosstalk is sufficient for the metabolic or EMT circuits to gain tristability. Further, activating multiple crosstalks is sufficient to drive the system fully towards the E/M-W/O state and suppress all other coupled phenotypes suggesting EMT and metabolic reprogramming are strong coupled and mutually drive the system towards a highly aggressive cancer phenotype. We also confirmed stabilizing the hybrid E/M state, using the phenotypic stability factors (PSFs) GRHL2 and OVOL2 [39,40], and upregulating the W/O state, using GRHL2 [41], further stabilized the E/M-W/O state for all sets of active crosstalks compared to the coupled tristable network.

Model

While the mechanisms of EMT and cancer metabolism have been investigated individually, the crosstalk between the two circuits and how the phenotypes are correlated is still largely unknown. Here we couple the EMT [7] and metabolic [22] regulatory networks (see Figure 1A for the coupled network). Our model includes the production, degradation, and

regulatory terms of the two individual networks and introduces crosstalk between them. We only consider crosstalks between components of the core circuits; therefore, modeling of the crosstalks is independent of whether it is an indirect or direct regulation.

Starting with the miRNA crosstalks, by targeting and downregulating NRF2, the elimination of ROS is reduced by μ_{34} [42–44]. ROS production may also be upregulated through μ_{34} downregulating SOD2 [45] or via the p53 pathway [46,47]. This increase in ROS levels is potentially more pronounced in mitochondrial ROS (mtROS) than NADPH oxidase mediated ROS (noxROS) [42] and has recently been indicated as a factor in cancer drug resistance [48]. The crosstalk between Hif1 and μ_{200} family members can either upregulate or downregulate Hif1 expression [49]. While mir-429 upregulates Hif1, both mir-200b [50] and mir-200c [51] downregulate Hif1 expression. Further, there is a negative regulatory feedback loop between mir-200b and Hif1[50]. The inhibition of mir-200b by Hif-1 is indirect through upregulation of the downstream target ASCL2 [50]. Our coupled model only includes a mutual inhibitory feedback between μ_{200} and Hif1. Additionally, HIF1 can upregulate Snail[52]. The production of Snail is also regulated by AMPK through an inhibitory crosstalk[53]. AMPK also represses the production of Zeb1 [54]. Additionally, AMPK indirectly increases the production of μ_{200} by upregulating Sirt1 which downregulates the creb cycle and therefore μ_{200} [55–58].

The model of the two core circuits is generalized to include these crosstalks. The coupled network is modeled as a set of ordinary differential equations (ODEs). Transcriptional regulations (represented as solid lines in Figure 1A) are modeled as a shifted Hill function that up/downregulates either the production or degradation term based on experimental results. For the shifted Hill function, once the threshold of the regulator is achieved, the foldchange (λ) essentially becomes a multiplier of the production or degradation term (details in SI section 1.1).

The miRNA regulatory links (represented as dashed lines in Figure 1A) are modeled through three functions that reflect the steps of translation. The functions Y_μ, Y_m, and L represent the active miRNA degradation rate, active mRNA degradation rate, and translation rate (details in SI section 1.2). Lastly, within the metabolic regulatory network there is competitive regulation of ROS by Hif1 and AMPK which is modeled by a competition function similar to the shifted Hill function (details in SI section 1.3). The full equations for all components of the circuit are given in SI Section 1.4 and the parameters along with a brief explanation are given in SI Section 1.5. Unless specified, all crosstalks are assumed to be in the inactive state (the foldchange, λ, of the crosstalk is equal to one and there is no miRNA regulation of Hif1 by μ_{200} by setting the value of $\mu_{200} = 0$ such that $L_h(\mu_{200} = 0) = 1$, $Y_{m,h}(\mu_{200} = 0) = 0$, and $Y_{\mu,h}(\mu_{200} = 0) = 0$).

We initially only include crosstalks between the core networks, then we investigate whether these crosstalks are sufficient to generate the hybrid states (details in SI Section 1.6). Lastly, we evaluate the PSFs OVOL and GRHL2 to determine stability of the E/M-W/O state (details and rate equations in SI Section 1.7).

Results

Coupling the EMT and metabolic regulatory networks results in nine possible coupled states

Individually, the EMT and metabolic regulatory networks are tristable with stable states (E, M, and E/M) and (W, O, and W/O), respectively (see Fig S1 for nullclines, section S2.5). By including the crosstalks, we identify how the components of the networks interact and which states are coupled. When the networks are coupled but the regulations are inactive, there are nine

possible couplings of the EMT and metabolic phenotypes: E-W, E-O, E-W/O, M-W, M-O, M-W/O, E/M-W, E/M-O, and E/M-W/O (Fig 1B, details of simulation in section S2.1).

While the Warburg state is characterized as high/low Hif1/AMPK expression and the Epithelial state is characterized as high/low μ_{200}/Zeb mRNA expression, the crosstalks may alter the expression profiles for the steady states such that the thresholds of the steady states change. Therefore, we use a distance metric normalized by the expression of the inactive network to classify the generated expression profiles as one of the nine coupled states (see Section S2.2 for details). With our coupled network parameters, the results stabilize at 1000 initial conditions - the hybrid state is most populous (W/O and E/M) followed by the W and M phenotypes, with the fewest initial conditions leading to the O and E states (Fig S3-S5). This is just one set of parameters and others may lead to a different fraction of initial conditions leading to these states.

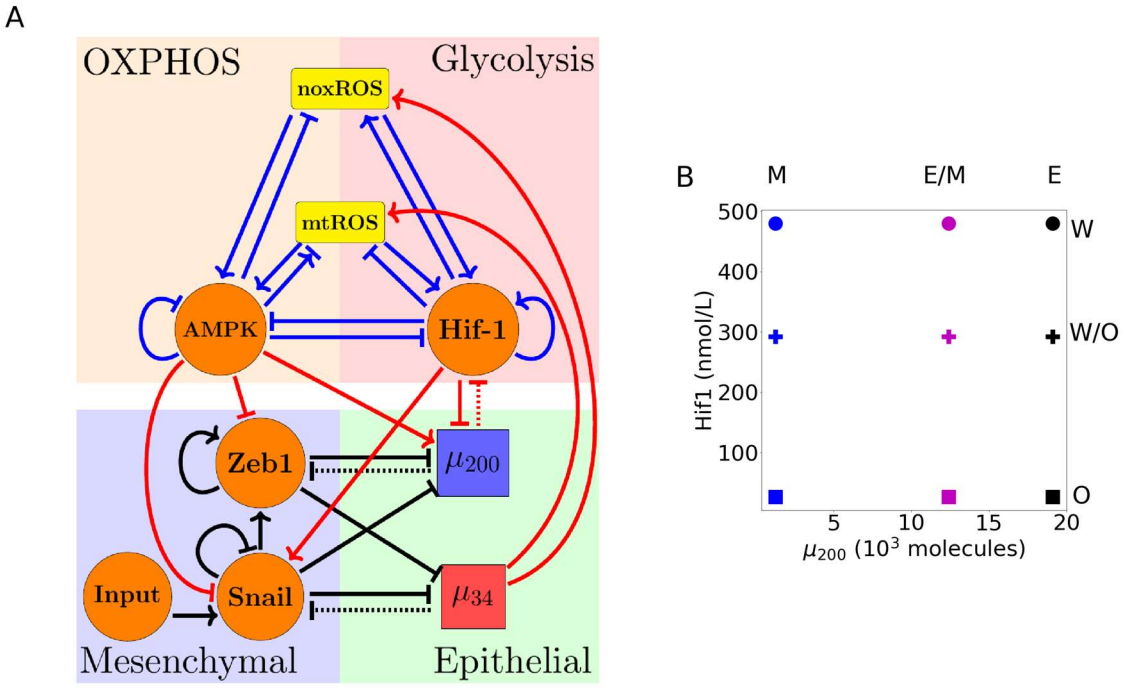

Figure 1. **The coupled EMT/MR circuit results in 9 coupled steady states. (A)** The network showing the core EMT module (bottom) with regulatory links designated by black, the core metabolic circuit (top) with regulatory links designated by blue, and the crosstalks noted in red. The dashed lines denote miRNA

regulation rather than transcriptional regulation. Regulatory links ending in bars represent inhibition while the arrows represent activation links. **(B)** The 9 possible coupled states when all crosstalks are present and inactive. The blue, purple, and black markers represent the mesenchymal (M), hybrid epithelial-mesenchymal (E/M), and epithelial (E) steady states, respectively. The circle, cross, and square represent the Warburg (W), hybrid Warburg-OXPHOS (W/O), and OXPHOS (O) metabolic phenotypes, respectively. The coupled E/M-W/O state is therefore represented as a purple cross.

Individual crosstalks push regulated half of circuit towards a single state

Based on the network and crosstalks in Fig 1A, it would be assumed that AMPK (which downregulates Snail and Zeb while upregulating μ_{200}) should push the system towards epithelial while Hif1 (which downregulates μ_{200} and upregulates Snail) should push the system towards mesenchymal. Additionally, μ_{200} should downregulate Hif1 resulting in an inhibition of the Warburg and hybrid W/O states. Lastly, μ_{34} upregulating ROS is not as clear and may stabilize the hybrid W/O state. If a single crosstalk is slowly increased/decreased, a clear progression from all nine coupled states to the saturation of a single state is expected.

The miRNA of the EMT network can stabilize the W/O metabolic phenotype

When noxROS is upregulated by μ_{34} (Fig 2A), the hybrid W/O state is upregulated along with the coupled E/M-W/O phenotype. As the level of noxROS increases (μ_{34} upregulates noxROS by reducing the degredation), the possible coupled states reduce from all nine, losing first the E-W, then the E/M-W, and finally losing the M-W state (Fig 2B, section S2.4). Since only the Warburg state is fully suppressed at maximum upregulation ($\lambda_{\mu_{34},noxROS} = 0$), analyzing the percent of initial conditions that lead to the metabolic phenotype shows the lost coupled states associated with the Warburg phenotype are pushed towards the W/O phenotype but no change occurs for the OXPHOS associated states(Fig 2C). As there is no regulation on the EMT network, the total number of E, E/M, and M states are constant but the E/M state is more likely to be associated with the hybrid W/O metabolic phenotype (Fig 2D). Analyzing the states

coupled with the Warburg phenotype, however, shows the mesenchymal phenotype (M-W) persists longer (Fig 2E). Comparing to the upregulation of mtROS (Fig S6), the E-W and E/M-W states are also the first suppressed states. Additionally, upregulating mtROS is also correlated to an upregulation of the E/M-W/O phenotype. Further, activation of mtROS results in a downregulation of the OXPHOS metabolic phenotype alongside downregulation of the Warburg phenotype. Together, these results suggest ROS is critical to tumor progression, and mtROS may play a stronger role than noxROS.

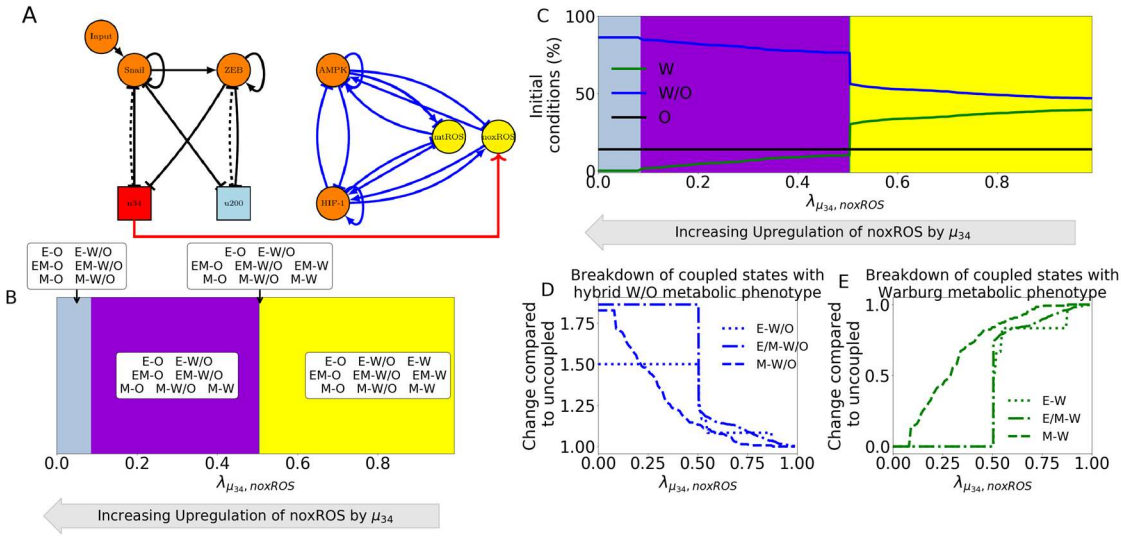

Figure 2. noxROS upregulated by mir34 results in upregulated W/O phenotype and associated with upregulated E/M-W/O phenotype. (A) A diagram of the core EMT circuit (left) and the core metabolic circuit (right) connected by the crosstalk between μ_{34} upregulating noxROS (red link representing transcriptional regulation). **(B)** Of the nine possible coupled states, as noxROS is upregulated by mir34, there are 4 distinct groupings. All possible couplings of the EMT phenotypes (E, M, and E/M) with both the O and W/O metabolic phenotypes persist for all levels of noxROS upregulation. The coupled states associated with the W metabolic phenotypes, (E-W, E/M-W, and M-W), are lost as the level of noxROS regulation increases for the lime, purple, and grey regions, respectively. **(C)** The background colors correspond to the colors representing the possible steady states of (B). The lines represent the total number of initial conditions leading to the W, O, or W/O phenotypes as a function of increasing regulation of noxROS by mir34. The W/O phenotype (blue) is upregulated, Warburg (green) phenotype is downregulated, and OXPHOS (black) is unchanged. **(D)** Showing the breakdown of the coupled states associated with the W/O phenotype (i.e., E-W/O, M-W/O, and E/M-W/O) compared to the inactive system ($\lambda_{\mu_{34},\mathrm{noxROS}} = 1$). The E/M-W/O coupled state is greatly upregulated once $\lambda_{\mu_{34},\mathrm{noxROS}} = 0.5$, the M-W/O coupled state is slowly upregulated, and E-W/O is also upregulated. **(E)** Same as (D) but for the coupled states associated with the Warburg phenotype. Once $\lambda_{\mu_{34},\mathrm{noxROS}} = 0.5$, both the E-W and M-W states are fully suppressed. The E/M-W coupled state continues to be downregulated until it is fully suppressed near $\lambda_{\mu_{34},\mathrm{noxROS}} = 0.1$.

If we want to determine how both miRNAs of the EMT network drive the metabolism network, and specifically the E/M-W/O state, we can first look at only the metabolic phenotypes. While upregulating ROS pushes the system towards the hybrid W/O metabolic phenotype, μ_{200} silencing Hif1 mRNA results in first the hybrid W/O phenotype being suppressed and then the Warburg phenotype being suppressed, leaving only OXPHOS as a possible metabolism (Fig 3A, detail of silencing function $P_H(\mu)$ in section S2.3). As mentioned previously, if ROS is upregulated than the W/O phenotype is upregulated (Fig 3B). Given the similar behavior between noxROS and mtROS, when either is active alongside μ_{200} downregulating Hif1 there are regions in which the hybrid W/O and coupled E/M-W/O states are fully suppressed (Fig S?). If both noxROS and mtROS are upregulated by μ_{34} the E/M-W/O state is further upregulated (Fig S?). Interestingly, if all three miRNA crosstalks are active (Fig 3C) the W/O state is present, but the E/M-W/O coupled state may be suppressed (Fig 3D). The E/M-W/O phenotype is present for all values of noxROS upregulation but is only present at high values of mtROS upregulation, suggesting a feedback loop between mtROS, HIf1 and μ_{200} controls the expression of the E/M-W/O state.

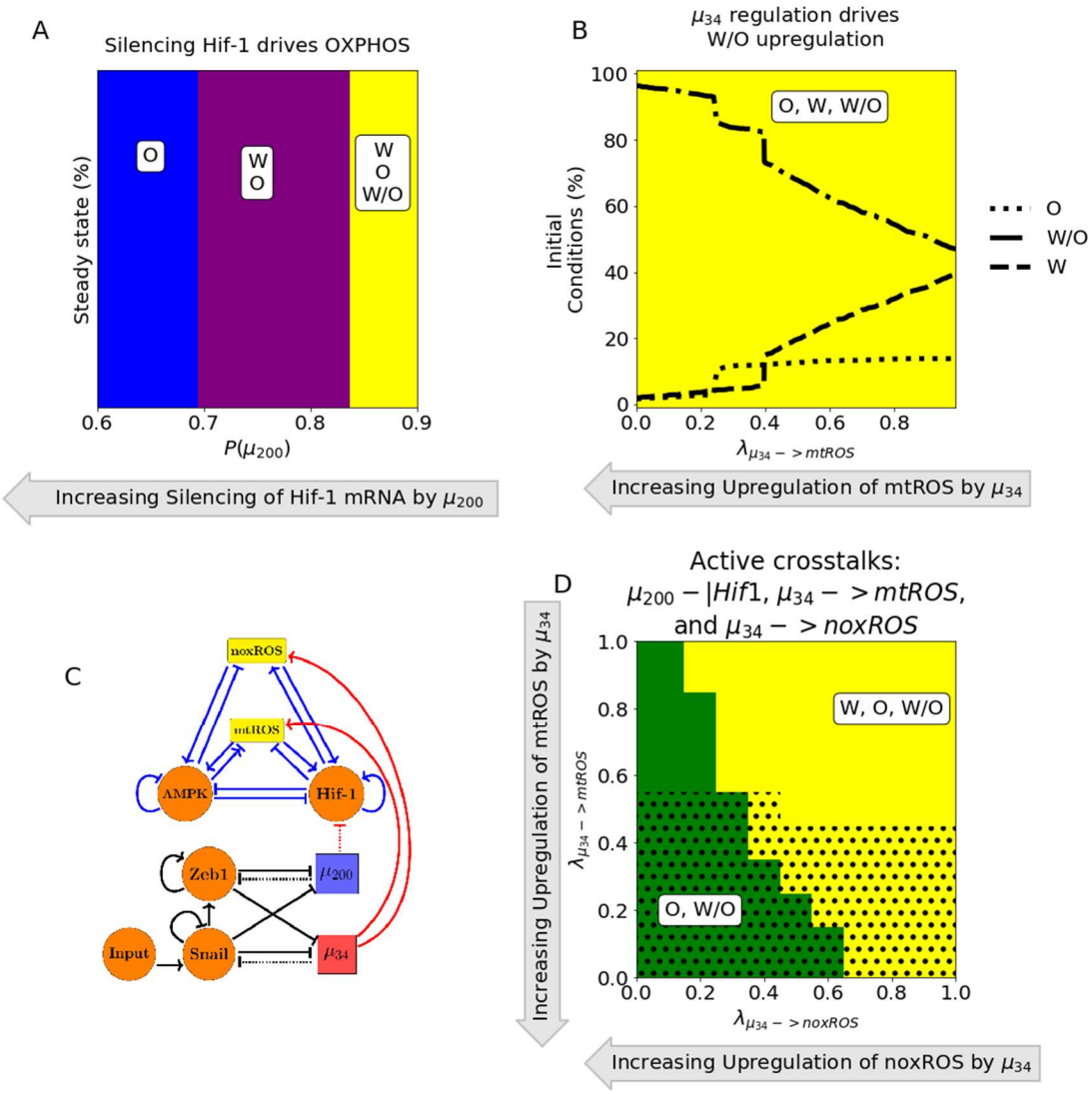

Figure 3. miRNA of the EMT regulatory network can upregulate the W/O phenotype. (A) The metabolic phenotypes associated with increasing silencing of the Hif-1 mRNA by μ_{200}. The colors (blue, purple, and yellow) represent the regions with possible phenotypes (O, [W,O], and [W,O,W/O]). The hybrid W/O state is suppressed first, then the Warburg state, and only OXPHOS is a possible metabolic phenotype when Hif-1 mRNA has been mostly silenced. **(B)** The affect of μ_{34} upregulating mtROS on the available metabolic phenotypes. As mtROS is upregulated the OXPHOS and Warburg phenotypes are slowly suppressed and at maximum upregulation ($\lambda_{\mu_{34},mtRO} = 0$) over 95% of initial conditions lead to the hybrid W/O phenotype. **(C)** The coupled metabolic (top) and EMT (bottom) regulatory network with all EMT driven regulatory links active (μ_{34} upregulating mtROS, μ_{34} upregulating noxROS, and μ_{200} silencing Hif-1). **(D)** The phase plane corresponding to all EMT driven regulatory links (network pictured in C). The regulation of Hif-1 by μ_{200} in this phase plane corresponds to the yellow region of (A) where all metabolic phenotypes are possible. As noxROS is upregulation (right to left), the Warburg metabolic phenotype is suppressed. However, as the level of mtROS increases (top to bottom), the black dotted region appears showing the existence of the E/M-W/O coupled state, suggesting mtROS may have a stronger affect on the E/M-W/O phenotype than noxROS.

TFs of the metabolic network can stabilize the E/M metabolic phenotype

To elucidate the way in which metabolic reprogramming drives EMT, we determine the affect of each metabolism driven crosstalk on the coupled states. Looking more closely at the crosstalks in which Hif-1 regulates Snail and μ_{200}, we see they push the system towards the mesenchymal state. Further, both the epithelial and hybrid E/M states are most associated with the OXPHOS metabolic state while the mesenchymal state is initially associated with the Warburg state. Interestingly, when Hif-1 regulates the EMT circuit, the E-O and E/M-O coupled states persist, with the E/M-O existing at more values of the foldchange than the E-O state. Opposite to Hif-1 driven crosstalks, AMPK pushes the EMT network to adopt an epithelial phenotype and suppresses the E/M state before the mesenchymal state. Additionally, if AMPK is regulating the EMT circuit, the epithelial and mesenchymal states are still most associated with the OXPHOS and Warburg metabolic phenotypes, respectively, but the E/M state is associated with the Warburg state. A different metabolic phenotype associated with the hybrid E/M depending on the crosstalk suggests neither OXPHOS nor Warburg metabolism is strongly associated with the E/M phenotype. Furthermore, AMPK inhibiting Zeb or Snail have nearly identical phases (Fig S7 and S11) but AMPK upregulating μ_{200} goes through different sets of possible steady states before saturating at fully epithelial (Fig S8). Similarly, Hif1 inhibiting μ_{200} and Hif1 upregulating Snail go through different sets of possible steady states before nearly saturating at mesenchymal (Figs S10 and S9).

There are two distinct events at play when the metabolic network regulates the EMT circuit. AMPK regulation quickly suppresses the E/M phenotype and pushes the system towards the Epithelial state whereas Hif1 regulation can allow the system to maintain the E/M phenotype while ultimately pushing the system towards mesenchymal (Fig 4A and 4B). Further, modulating the input to Snail can alter the location of the E/M state (see Fig S12). As AMPK and Hif1 push

the system towards opposite states, having one of each would suggest the circuit would be pushed toward hybrid. That is exactly what happens for any combination of the three AMPK crosstalks and two Hif1 crosstalks, although the exact values of where the E/M-W/O state exists depends on the type of regulation (Fig S?). Additionally, if AMPK and Hif-1 target different EMT TFs, the E/M-W/O state may exist in more regions than if they target the same TF (Fig S?), suggesting multiple crosstalks must be active to stabilize the E/M-W/O state. If all crosstalks involving AMPK and Hif1 regulating the EMT circuit are active (Fig 4C) then there are regions in which the E/M state exists (Fig 4D). However, when analyzing the system for the existence of the E/M-W/O phenotype, it only exists in smaller regions compared to full regulation of the metabolism network (the black dotted regions of Fig 4D compared to Fig 3D).

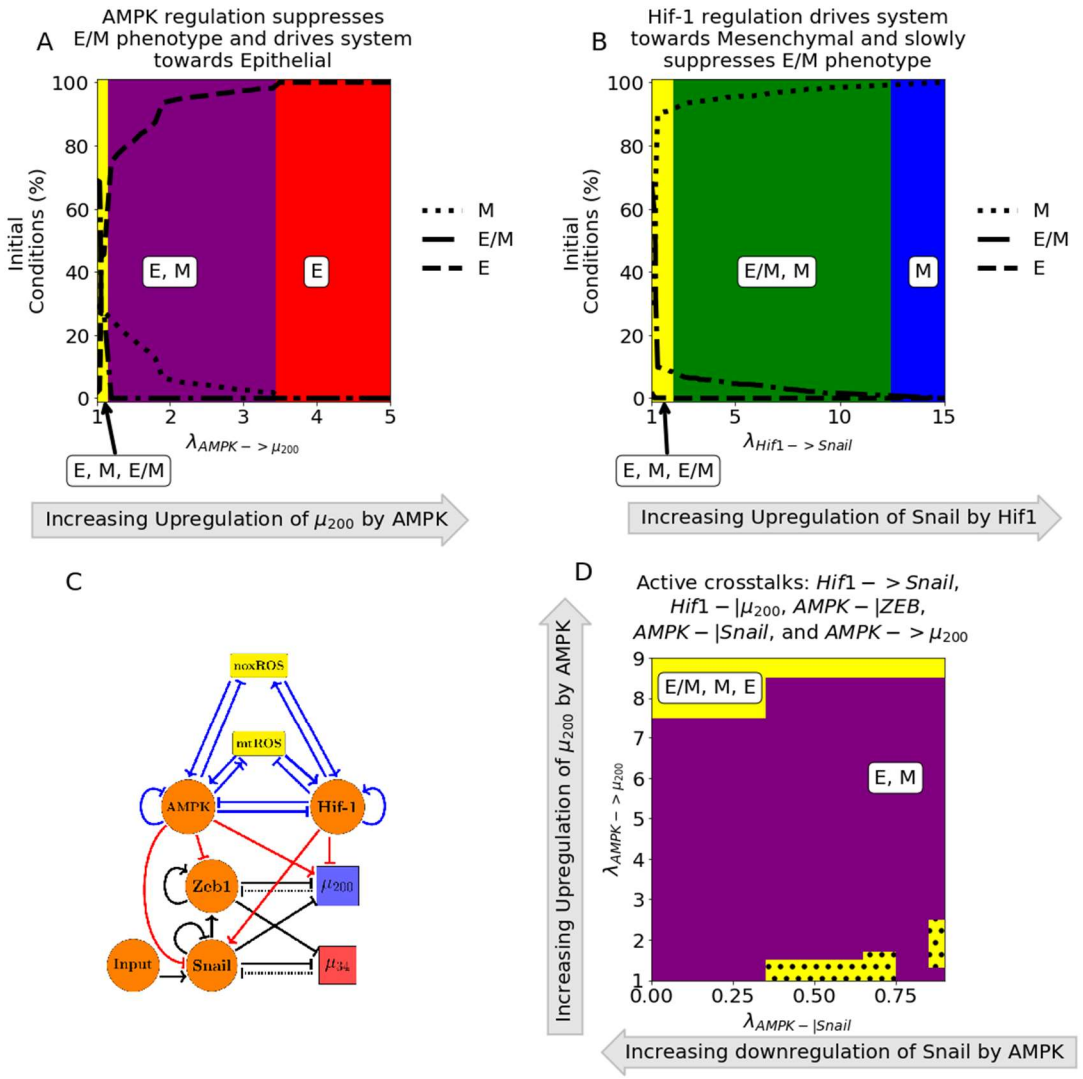

Figure 4. AMPK and Hif-1 cooperate to upregulate the hybrid E/M state. (A) The number of initial conditions leading to an E/M, M, or E phenotype as AMPK upregulates μ_{200}. The hybrid E/M phenotype is suppressed quickly as the system is driven towards epithelial. **(B)** Similar to (A) but for Hif-1 driving the system towards mesenchymal. The E/M state persists longer for Hif-1 regulation than AMPK. **(C)** The network showing metabolism driven crosstalks. Zeb is inhibited by AMPK, Snail is upregulated by Hif-1 while being downregulated by AMPK, and μ_{200} is upregulated by AMPK while being inhibited by Hif-1. **(D)** The phases plane of potential EMT phenotypes when all metabolic driven crosstalks are active. When all five crosstalks are actively regulating the EMT circuit, there are only a few regions where the E/M phenotype exists alongside the E and M phenotype (yellow regions). Additionally, there are some regions (the dotted black areas) where the E/M-W/O coupled state also exists.

Hybrid E/M-W/O phenotype can be stabilized

As the most aggressive cancers phenotypes are characterized by the hybrid states of both the EMT and metabolism networks, we narrow our search onto how the crosstalks in both

directions affect the presence of the E/M-W/O state and the behavior of the coupled states as the regulatory crosstalks change.

Identifying the phases present when all metabolism regulating crosstalks (μ_{200} silencing HIf1 mRNA and μ_{34} upregulating noxROS and mtROS) are active shows the E/M-W/O state is suppressed when mtROS is only slightly upregulated (Fig. 5a shows the coupled states corresponding to the metabolic phenotypes in Fig 3C). Further, the epithelial and E/M states are associated with the OXPHOS phenotype when mtROS levels are slightly upregulated. Interestingly, the mesenchymal state is coupled with O and W/O metabolic phenotypes while the E and E/M states are only coupled to the W/O phenotype when mtROS is fully upregulated. The upregulation of the E/M-W/O phenotype as the mtROS levels increase suggests ROS is necessary for the EMT.

To stabilize the E/M state an AMPK and Hif1 crosstalk are necessary, and if all EMT regulating crosstalks are active then there are regions where the E/M-W/O state exists. Additionally, the epithelial state is typically coupled to OXPHOS metabolism (E-O), the mesenchymal state is associated with the Warburg metabolic phenotype (M-W), and when the E/M state is present it is associated with the hybrid metabolic phenotype (Fig 5B). In fact, for any system, if there are only three coupled states available and each has a distinct phenotype of the EMT and metabolic networks than the only possible set of states is E-O, M-W, and E/M-W/O. This suggests, cells in the primary tumor utilize OXPHOS while clusters of migrating cells utilize a combination of aerobic glycolysis and OXPHOS.

To stabilize and upregulate the E/M-W/O state one would expect ROS must be upregulated and two competing crosstalks regulating the EMT network would be needed. The

E/M-W/O state is upregulated if these conditions are met and can even be upregulated for small ranges of parameters if there is one crosstalk in both directions. Interestingly, with just three regulations (Hif1 inhibiting μ_{200}, μ_{34} upregulating mtROS, and modulating the input to Snail) all states except the hybrid E/M-W/O state can be suppressed (Fig 5C). This region persists even if all crosstalks are active (Fig 5D). Further, the other phases present with these active crosstalks are the same, suggesting there is a progression that must be followed to generate the E/M-W/O state. Additionally, the persistence of the E/M-W/O state suggests there are other combinations of crosstalks that generate phases where only the E/M-W/O state is possible, although it is outside the scope of this manuscript to find all possible combinations of crosstalks that can suppress all states except the hybrid E/M-W/O coupled state.

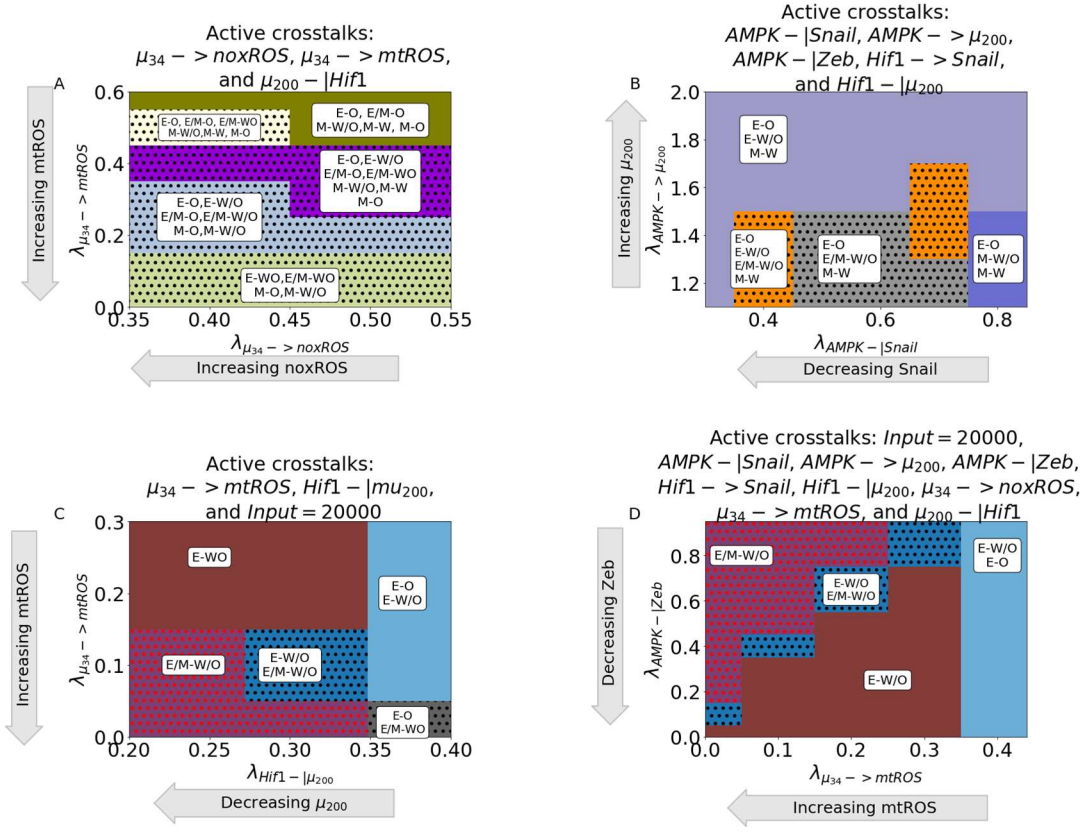

Figure 5. The EMT and metabolic regulatory networks crosstalks can drive the system to the hybrid E/M-W/O coupled state. (A) The coupled states when only EMT driven crosstalks are active

(μ_{200} downregulating Hif1 and μ_{34} upregulating mtROS and noxROS). The E/M-W/O state exists when mtROS is upregulated. **(B)** The coupled states when only TFs and miRNAs of the EMT circuit are regulated by TFs of the metabolic circuit (AMPK-|Snail, AMPK-|Zeb, AMPK->u200, Hif1-|u200, Hif1->Snail). The results suggest a correlation between the E, E/M, and M phenotypes to the O, W/O, and W metabolic phenotypes. **(C)** When crosstalks mutually drive EMT and metabolic reprogramming, there are parameter spaces in which the only possible coupled state is the E/M-W/O state. **(D)** When all crosstalks are active there are regions where only the E/M-W/O state exists. Similar sets of coupled states in (C) and (D) suggest a preferential pathway to drive the system towards the hybrid E/M-W/O coupled state.

Normal cells can become cancerous when crosstalks introduced

We have confirmed that the E/M and W/O states are coupled, the E/M-W/O state can be upregulated, and there are parameter sets with only the hybrid E/M-W/O state available and all other coupled states suppressed. Now we determine whether the crosstalks are strong enough to generate the hybrid states. The model of the previous sections was for the tristable circuits so we modified the parameters to ensure each circuit was initially bistable (i.e., only the E, M, W, and O states are possible). We confirmed the parameters of the inactive coupled system resulted in a bistable system by calculating the nullclines (Table S? for parameters that were changed compared with the coupled tristable systems and Fig S2, Fig S14-S15).

For the metabolic circuit, the system only becomes tristable at high levels of mtROS upregulation (Fig 6A). Additionally, when μ_{34} activates mtROS it can even upregulate the E/M-W/O state as compared to the initially tristable system with no active crosstalks. The system remains bistable if only noxROS is upregulated or Hif1 is downregulated (Fig S?). Furthermore, when looking at the crosstalks on the bistable EMT network (i.e., no E/M stable state) AMPK driven crosstalks cannot generate the E/M state but regulation by Hif1 or modulating the input to snail can (Fig 6B and S?). The EMT network can also attain tristability if there are two competing crosstalks, such as AMPK upregulating Snail and Hif-1 downregulating μ_{200}.

When comparing these results to the tristable circuit we can look at the simplest set of crosstalks with a parameter region that suppressed all coupled states except the E/M-W/O state (namely Hif-1 inhibiting μ_{200}, μ_{34} upregulating mtROS, and modulating the input to Snail). The results for the bistable circuit are qualitatively very similar to the tristable circuit (Fig 5C compared to Fig 6C). The E/M state is only possible near full inhibition of μ_{200} and the W/O state is possible when mtROS greatly upregulated. Further, the system must be near maximum regulation (i.e. both foldchanges must be close to zero) to generate the region where only the hybrid E/M-W/O coupled state is possible. The nearby phases correspond to the tristable circuit, further supporting the existence of a preferential pathway that stabilizes the E/M-W/O state and follows intuition. As EMT starts with an epithelial state, and knowing the epithelial state typically uses OXPHOS, the transition from E-O to E-W/O to E/M-W/O suggests metabolism may help drive EMT. These results suggest μ_{34} upregulating mtROS and Hif1 regulating EMT may stabilize the E/M-W/O state more than the other crosstalks.

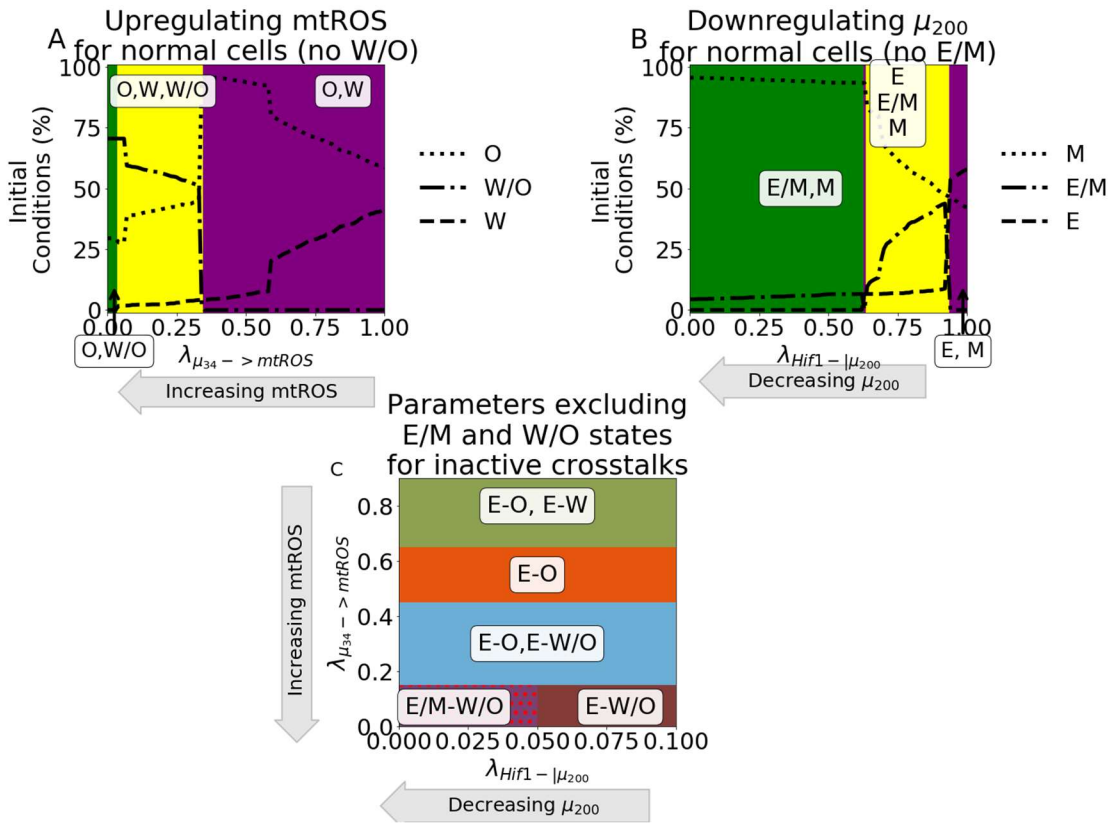

Figure 6. Parameter ranges which exclude the possibility of the hybrid state can be modulated by crosstalk to generate the hybrid state. (A) Our model using parameters that remove the hybrid W/O metabolic state from the steady state possibilities when the crosstalk is inactive ($\lambda_{\mu_{34}->\mathrm{mtROS}} = 1.$). Initially, only the OXPHOS and Warburg metabolic states can be accessed with an increase in the percent of OXPHOS steady states and decrease in Warburg phenotypes. Once $\lambda_{\mu 34} = 0.35$, there is a sharp change with the hybrid W/O phenotype becoming the most often occupied phenotype. **(B)** Our model using parameters that remove the hybrid E/M phenotype from the accessible states when the crosstalks are inactive. As the inhibition increases ($\lambda_{\mathrm{Hif1}-|\mu_{200}}$ goes towards zero), the system goes from only the E and M states available to regions in which the E/M phenotype is accessible. **(C)** Combining the models from (A) and (B), we generate a model which only has 4 possible coupled states if the crosstalks are inactive (E-O, E-W, M-O, and M-W). At maximum upregulation of mtROS and downregulation of μ_{200}, the E/M-W/O state is the only one accessible, similar to the model with parameters always allowing access to the E/M-W/O state (Fig. 5C).

PSFs stabilize the E/M state which stabilized W/O state

Lastly, we determined whether the E/M and W/O states could be further stabilized, and therefore upregulate the E/M-W/O state, by adding two protein stability factors GRHL2 and OVOL2 to the network. Both PSFs ensure the E/M state is stabilized and GRHL2 also

upregulates ROS (Fig 7A). The PSF stabilized coupled network with inactive crosstalks can either be in the E/M-W/O or E/M-O state (Fig S?).

When a single crosstalk is active in the PSF coupled network, the behavior is as expected with the E/M-W/O state persisting for more values than the tristable coupled network. When any of the Hif-1 driven crosstalks regulating the EMT circuit are active, there is an increased region in which the E/M-W/O state is possible (Fig S?). Further, if AMPK is regulating the EMT circuit than the E/M-W/O state is possible throughout the entire region analyzed for the tristable circuit (Fig S?).

When multiple crosstalks are active the stability of the E/M-W/O state persists. If two competing crosstalks on the EMT circuit are active (i.e., one Hif-1 and one AMPK driven regulation active), then the E/M-W/O state is possible for most of the parameter space (Fig 7B). The regulatory crosstalks controlled by Hif1 seem to have a stronger affect than the AMPK crosstalks, and can push the system towards mesenchymal. This follows the tristable coupled network where AMPK upregulating μ_{200} seems to have a weaker effect, specifically on the E/M-W/O state, than Hif1 downregulating μ_{200}. Lastly, we can compare the regions where E/M-W/O is the only state when μ_{34} upregulates mtROS, Hif1 downregulates μ_{200}, and the input to Snail is modulated. We see the state exists in a far larger region when stabilized by the PSFs than in the tristable coupled network (Fig 7C). Once again the phases close to the E/M-W/O only region are similar to the possible sets of coupled states that also exist for the same group of active crosstalks in the tristable circuit.

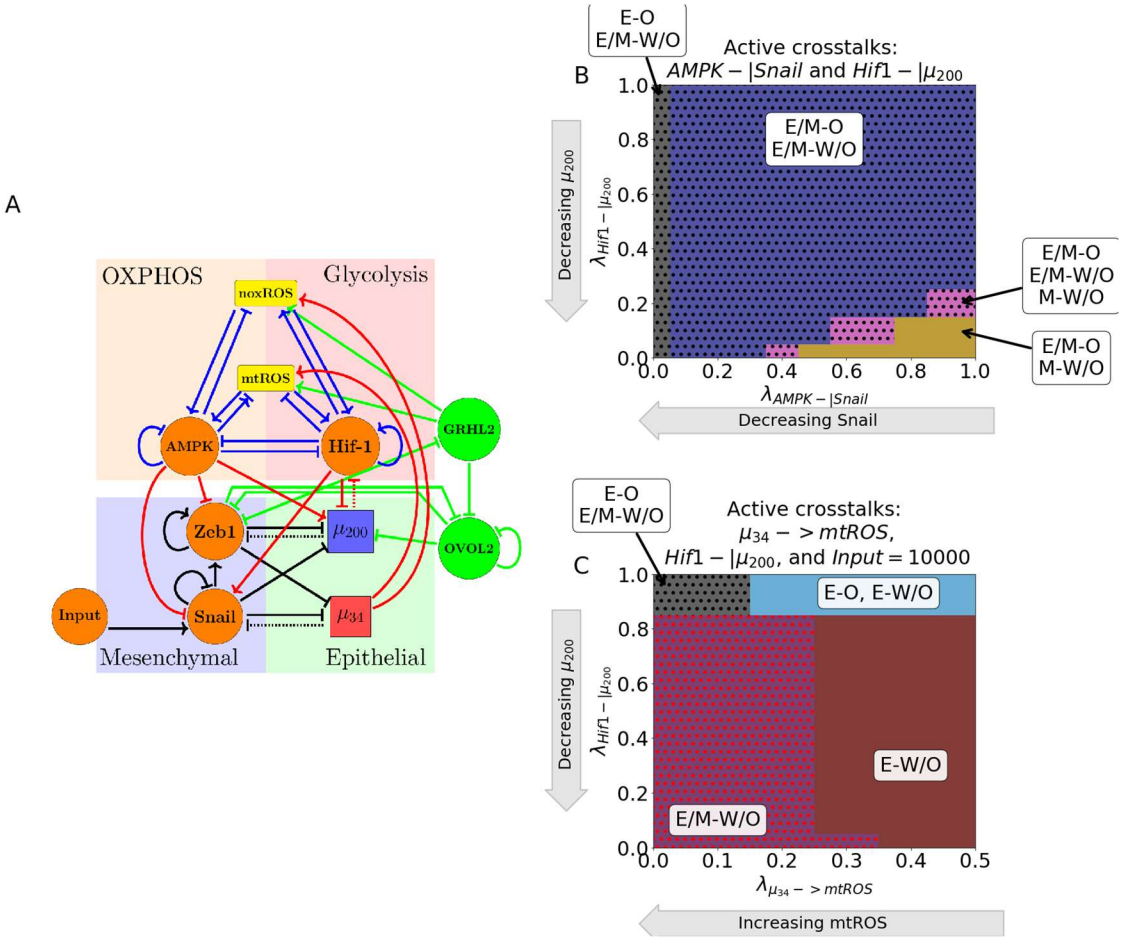

Figure 7. PSFs stabilizing E/M state can increase parameters spaces of E/M-W/O states. (A) The modified network to include GRHL2 and OVOL2. **(B)** The coupled E/M-W/O state is present in more of the space due to the PSFs stabilizing the E/M state even when AMPK downregulates Snail and Hif1 downregulated μ_{200}. **(C)** The phase space when the Input to Snail is set to 10K, μ_{34} is upregulating mtROS, and Hif1 is downregulating μ_{200}. There is a larger region where E/M-W/O is the only possible coupled state compared to the original model (see Fig 5C).

Discussion

Based on this work we have seen that there does seem to be a link between the hybrid E/M and W/O states suggesting that metastasizing cells require a hybrid approach to increase their rate of energy production. We have identified some crosstalks that could be expanded upon to increase our understanding of metastasis.

mtROS nearly suppressing the OXPHOS and Warburg phenotypes combined with the results that increase of EM/WO is more pronounced for mtROS than noxROS[42] suggests

mtROS specifically is critical to tumor progression. Recent work by Radisky and collaborators has suggested ROS may be important to begin the epithelial to mesenchymal transition [59]. Our results that Hif-1 crosstalks seem to be stronger than AMPK corresponds to the well-known role of hypoxia triggering the EMT [9]. Given Hif is important in metabolic reprogramming [19] and our results showing, in combination with other crosstalks, Hif-1 can stabilize the E/M-W/O state suggesting metabolic reprogramming may occur before EMT. Recently, the role of miRNAs in the cancer metastasis [60] has been emphasized and we have seen the role of μ_{34} upregulating ROS plays in triggering the W/O phenotype. Further, our results suggest metabolic reprogramming occurs before the EMT and suggests the existence of a feedback loop between μ_{34}, μ_{200}, Hif-1 and ROS that may be critical to stabilizing the E/M-W/O state associated with tumorigenesis.

The feedback loop, especially μ_{34} upregulating ROS, may be of critical importance given the two pathways mentioned previously, p53 and KEAP1-NRF2, may have competing effects on EMT and metabolism. For instance, there is a connection between NRF2 upregulation and the E/M phenotype [36] but NRF2 is also an antioxidant that must be downregulated to upregulate ROS production [42–44]. However, the metabolic phenotype of NRF2 stabilized E/M cells may correspond to a hybrid W/O phenotype [25]. The p53 pathway seems to upregulate noxROS [46,47]. Here we establish a connection between ROS upregulation and the E/M-W/O phenotype, and to further elucidate the mechanism by which ROS promotes tumorigenesis, additional pathways such as the KEAP1-NRF2 and p53 pathways should also be explored in conjunction with crosstalks between the EMT and metabolic circuits. Additionally, the E/M-W/O state was stabilized when the input to Snail was modulated confirming the tumor

microenvironment and other signals, such as TGF-β, may be important to generating the E/M-W/O state.

To stabilize only the E/M-W/O state, the system seems to first require the E-O state, then the E-W/O or E/M-O states, before stabilizing the E/M-W/O state and suppressing all other systems. This result suggests the mechanism to stabilize the E/M-W/O may be less about stabilizing the state and more about stopping the transition. Additionally, the E/M-W/O can be fully upregulated, and all other coupled states suppressed regardless of whether the system is initially near that state or not, suggesting the crosstalks involved in tumorigenesis have evolved to ensure survival and proliferation. Therefore, to cancer therapies should be developed that target the EMT pathway in conjunction with the metabolic pathway.

Acknowledgements

[1] D. Hanahan and R. A. Weinberg, *Hallmarks of Cancer: The Next Generation*, Cell **144**, 646 (2011).

[2] R. Kalluri, *EMT: When epithelial cells decide to become mesenchymal-like cells*, Journal of Clinical Investigation **119**, 1417 (2009).

[3] J. M. Lee, S. Dedhar, R. Kalluri, and E. W. Thompson, *The epithelial–mesenchymal transition: new insights in signaling, development, and disease*, The Journal of Cell Biology **172**, 973 (2006).

[4] M. Lu, M. K. Jolly, H. Levine, J. N. Onuchic, and E. Ben-Jacob, *MicroRNA-based regulation of epithelial–hybrid–mesenchymal fate determination*, Proceedings of the National Academy of Sciences **110**, 18144 (2013).

[5] M. Saitoh, *Involvement of partial EMT in cancer progression*, The Journal of Biochemistry **164**, 257 (2018).

[6] D. Bhattacharya, A. P. Azambuja, and M. Simoes-Costa, *Metabolic Reprogramming Promotes Neural Crest Migration via Yap/Tead Signaling*, Developmental Cell **53**, 199 (2020).

[7] O. Warburg, F. Wind, and E. Negelein, *THE METABOLISM OF TUMORS IN THE BODY*, Journal of General Physiology **8**, 519 (1927).

[8] M. V. Liberti and J. W. Locasale, *The Warburg Effect: How Does it Benefit Cancer Cells?*, Trends in Biochemical Sciences **41**, 211 (2016).

[9] L. Yu, M. Lu, D. Jia, J. Ma, E. Ben-Jacob, H. Levine, B. A. Kaipparettu, and J. N. Onuchic, *Modeling the Genetic Regulation of Cancer Metabolism: Interplay between Glycolysis and Oxidative Phosphorylation*, Cancer Research **77**, 1564 (2017).

[10] I. Georgakopoulos-Soares, D. V. Chartoumpekis, V. Kyriazopoulou, and A. Zaravinos, *EMT Factors and Metabolic Pathways in Cancer*, Frontiers in Oncology **10**, 499 (2020).

[11] D. Jia, J. H. Park, H. Kaur, K. H. Jung, S. Yang, S. Tripathi, M. Galbraith, Y. Deng, M. K. Jolly, B. A. Kaipparettu, J. N. Onuchic, and H. Levine, *Towards decoding the coupled decision-making of metabolism and epithelial-to-mesenchymal transition in cancer*, British Journal of Cancer 1 (2021).

[12] F. Bocci, S. C. Tripathi, S. A. V. Mercedes, J. T. George, J. P. Casabar, P. K. Wong, S. M. Hanash, H. Levine, J. N. Onuchic, and M. K. Jolly, *NRF2 activates a partial epithelial-mesenchymal transition and is maximally present in a hybrid epithelial/mesenchymal phenotype*, Integrative Biology **11**, 251 (2019).

[13] M. Luo, L. Shang, M. D. Brooks, E. Jiagge, Y. Zhu, J. M. Buschhaus, S. Conley, M. A. Fath, A. Davis, E. Gheordunescu, Y. Wang, R. Harouaka, A. Lozier, D. Triner, S. McDermott, S. D. Merajver, G. D. Luker, D. R. Spitz, and M. S. Wicha, *Targeting Breast Cancer Stem Cell State Equilibrium through Modulation of Redox Signaling*, Cell Metabolism **28**, 69 (2018).

[14] J. A. Colacino, E. Azizi, M. D. Brooks, R. Harouaka, S. Fouladdel, S. P. McDermott, M. Lee, D. Hill, J. Madden, J. Boerner, M. L. Cote, M. A. Sartor, L. S. Rozek, and M. S. Wicha, *Heterogeneity of Human Breast Stem and Progenitor Cells as Revealed by Transcriptional Profiling*, Stem Cell Reports **10**, 1596 (2018).

[15] S. Kovac, P. R. Angelova, K. M. Holmström, Y. Zhang, A. T. Dinkova-Kostova, and A. Y. Abramov, *Nrf2 regulates ROS production by mitochondria and NADPH oxidase*, Biochimica et Biophysica Acta (BBA) - General Subjects **1850**, 794 (2015).

[16] F. He, X. Ru, and T. Wen, *NRF2, a Transcription Factor for Stress Response and Beyond*, International Journal of Molecular Sciences **21**, 4777 (2020).

[17] N. Li, S. Muthusamy, R. Liang, H. Sarojini, and E. Wang, *Increased expression of miR-34a and miR-93 in rat liver during aging, and their impact on the expression of Mgst1 and Sirt1*, Mechanisms of Ageing and Development **132**, 75 (2011).

[18] X.-Y. Bai, Y. Ma, R. Ding, B. Fu, S. Shi, and X.-M. Chen, *miR-335 and miR-34a Promote Renal Senescence by Suppressing Mitochondrial Antioxidative Enzymes*, Journal of the American Society of Nephrology **22**, 1252 (2011).

[19] F. Navarro and J. Lieberman, *miR-34 and p53: New Insights into a Complex Functional Relationship*, PLoS ONE **10**, (2015).

[20] D. Italiano, A. M. Lena, G. Melino, and E. Candi, *Identification of NCF2/p67phox as a novel p53 target gene*, Cell Cycle **11**, 4589 (2012).

[21] H.-L. Chou, Y. Fong, C.-K. Wei, E.-M. Tsai, J. Y.-F. Chen, W.-T. Chang, C.-Y. Wu, H.-W. Huang, and C.-C. Chiu, *A Quinone-Containing Compound Enhances Camptothecin-Induced Apoptosis of Lung Cancer Through Modulating Endogenous ROS and ERK Signaling*, Archivum Immunologiae et Therapiae Experimentalis **65**, 241 (2017).

[22] M. Serocki, S. Bartoszewska, A. Janaszak-Jasiecka, R. J. Ochocka, J. F. Collawn, and R. Bartoszewski, *miRNAs regulate the HIF switch during hypoxia: a novel therapeutic target*, Angiogenesis **21**, 183 (2018).

[23] Y. Shang, H. Chen, J. Ye, X. Wei, S. Liu, and R. Wang, *HIF-1a/Ascl2/miR-200b regulatory feedback circuit modulated the epithelial-mesenchymal transition (EMT) in colorectal cancer cells*, Experimental Cell Research **360**, 243 (2017).

[24] Y. Byun, Y.-C. Choi, Y. Jeong, G. Lee, S. Yoon, Y. Jeong, J. Yoon, and K. Baek, *MiR-200c downregulates HIF-1a and inhibits migration of lung cancer cells*, Cellular & Molecular Biology Letters **24**, 28 (2019).

[25] X. Xu, X. Tan, B. Tampe, E. Sanchez, M. Zeisberg, and E. M. Zeisberg, *Snail Is a Direct Target of Hypoxia-inducible Factor 1a (HIF1a) in Hypoxia-induced Endothelial to Mesenchymal Transition of Human Coronary Endothelial Cells**, Journal of Biological Chemistry **290**, 16653 (2015).

[26] C.-C. Chou, K.-H. Lee, I.-L. Lai, D. Wang, X. Mo, S. K. Kulp, C. L. Shapiro, and C.-S. Chen, *AMPK Reverses the Mesenchymal Phenotype of Cancer Cells by Targeting the Akt–MDM2–Foxo3a Signaling Axis*, Cancer Research **74**, 4783 (2014).

[27] J. Ohshima, Q. Wang, Z. R. Fitzsimonds, D. P. Miller, M. N. Sztukowska, Y.-J. Jung, M. Hayashi, M. Whiteley, and R. J. Lamont, *Streptococcus gordonii programs epithelial cells to resist ZEB2 induction by Porphyromonas gingivalis*, Proceedings of the National Academy of Sciences **116**, 201900101 (2019).

[28] W. Huang, J. Cao, X. Liu, F. Meng, M. Li, B. Chen, and J. Zhang, *AMPK Plays a Dual Role in Regulation of CREB/BDNF Pathway in Mouse Primary Hippocampal Cells*, Journal of Molecular Neuroscience **56**, 782 (2015).

[29] H. Jin, L. Xue, L. Mo, D. Zhang, X. Guo, J. Xu, J. Li, M. Peng, X. Zhao, M. Zhong, D. Xu, X.-R. Wu, H. Huang, and C. Huang, *Downregulation of miR-200c stabilizes XIAP mRNA and contributes to invasion and lung metastasis of bladder cancer*, Cell Adhesion & Migration **13**, 236 (2019).

[30] M. Janin and M. Esteller, *Oncometabolite Accumulation and Epithelial-to-Mesenchymal Transition: The Turn of Fumarate*, Cell Metabolism **24**, 529 (2016).

[31] Q. Zhang, S. Zheng, S. Wang, W. Wang, H. Xing, and S. Xu, *Chlorpyrifos induced oxidative stress to promote apoptosis and autophagy through the regulation of miR-19a-AMPK axis in common carp*, Fish & Shellfish Immunology **93**, 1093 (2019).

[32] D. C. Radisky, D. D. Levy, L. E. Littlepage, H. Liu, C. M. Nelson, J. E. Fata, D. Leake, E. L. Godden, D. G. Albertson, M. A. Nieto, Z. Werb, and M. J. Bissell, *Rac1b and reactive oxygen species mediate MMP-3-induced EMT and genomic instability*, Nature **436**, 123 (2005).

[33] K. Saxena, M. K. Jolly, and K. Balamurugan, *Hypoxia, partial EMT and collective migration: Emerging culprits in metastasis*, Translational Oncology **13**, 100845 (2020).

[34] G. Babaei, N. Raei, A. T. milani, S. G.-G. Aziz, N. Pourjabbar, and F. Geravand, *The emerging role of miR-200 family in metastasis: focus on EMT, CSCs, angiogenesis, and anoikis*, Molecular Biology Reports **48**, 6935 (2021).

[35] V. S. LeBleu, J. T. O'Connell, K. N. G. Herrera, H. Wikman, K. Pantel, M. C. Haigis, F. M. de Carvalho, A. Damascena, L. T. D. Chinen, R. M. Rocha, J. M. Asara, and R. Kalluri, *PGC-1a mediates mitochondrial biogenesis and oxidative phosphorylation in cancer cells to promote metastasis*, Nature Cell Biology **16**, 992 (2014).

1. Hanahan D. Hallmarks of Cancer: New Dimensions. Cancer Discov. 2022;12(1):31–46.

2. Kalluri R. EMT: When epithelial cells decide to become mesenchymal-like cells. J Clin Invest. 2009;119(6):1417–9.

3. Hay ED. The mesenchymal cell, its role in the embryo, and the remarkable signaling mechanisms that create it. Dev Dynam. 2005;233(3):706–20.

4. Pietilä M, Ivaska J, Mani SA. Whom to blame for metastasis, the epithelial–mesenchymal transition or the tumor microenvironment? Cancer Lett. 2016;380(1):359–68.

5. Talbot LJ, Bhattacharya SD, Kuo PC. Epithelial-mesenchymal transition, the tumor microenvironment, and metastatic behavior of epithelial malignancies. Int J Biochem Mol Biol. 2012 May 18;3(2):117–36.

6. Cho ES, Kang HE, Kim NH, Yook JI. Therapeutic implications of cancer epithelial-mesenchymal transition (EMT). Arch Pharm Res. 2019;42(1):14–24.

7. Lu M, Jolly MK, Levine H, Onuchic JN, Ben-Jacob E. MicroRNA-based regulation of epithelial–hybrid–mesenchymal fate determination. Proc National Acad Sci. 2013;110(45):18144–9.

8. Saitoh M. Involvement of partial EMT in cancer progression. J Biochem. 2018;164(4):257–64.

9. Saxena K, Jolly MK, Balamurugan K. Hypoxia, partial EMT and collective migration: Emerging culprits in metastasis. Transl Oncol. 2020;13(11):100845.

10. Bakir B, Chiarella AM, Pitarresi JR, Rustgi AK. EMT, MET, Plasticity, and Tumor Metastasis. Trends Cell Biol. 2020;30(10):764–76.

11. Pastushenko I, Blanpain C. EMT Transition States during Tumor Progression and Metastasis. Trends Cell Biol. 2018;29(3):212–26.

12. Fustaino V, Presutti D, Colombo T, Cardinali B, Papoff G, Brandi R, et al. Characterization of epithelial-mesenchymal transition intermediate/hybrid phenotypes associated to resistance to EGFR inhibitors in non-small cell lung cancer cell lines. Oncotarget. 2017;8(61):103340–63.

13. George JT, Jolly MK, Xu J, Somarelli J, Levine H. Survival outcomes in cancer patients predicted by a partial EMT gene expression scoring metric. Cancer Res. 2017;77(22):canres.3521.2016.

14. Dey P, Kimmelman AC, DePinho RA. Metabolic Codependencies in the Tumor Microenvironment. Cancer Discov. 2021;candisc.1211.2020.

15. Warburg O, Wind F, Negelein E. THE METABOLISM OF TUMORS IN THE BODY. J Gen Physiol. 1927;8(6):519–30.

16. Liberti MV, Locasale JW. The Warburg Effect: How Does it Benefit Cancer Cells? Trends Biochem Sci. 2016;41(3):211–8.

17. Ohshima K, Morii E. Metabolic Reprogramming of Cancer Cells during Tumor Progression and Metastasis. Metabolites. 2021;11(1):28.

18. Carvalho TMA, Cardoso HJ, Figueira MI, Vaz CV, Socorro S. The peculiarities of cancer cell metabolism: A route to metastasization and a target for therapy. Eur J Med Chem. 2019;171:343–63.

19. Nagao A, Kobayashi M, Koyasu S, Chow CCT, Harada H. HIF-1-Dependent Reprogramming of Glucose Metabolic Pathway of Cancer Cells and Its Therapeutic Significance. Int J Mol Sci. 2019;20(2):238.

20. Cheng Y, Lu Y, Zhang D, Lian S, Liang H, Ye Y, et al. Metastatic cancer cells compensate for low energy supplies in hostile microenvironments with bioenergetic adaptation and metabolic reprogramming. Int J Oncol. 2018;53(6):2590–604.

21. Jia D, Park JH, Jung KH, Levine H, Kaipparettu BA. Elucidating the Metabolic Plasticity of Cancer: Mitochondrial Reprogramming and Hybrid Metabolic States. Cells. 2018;7(3):21.

22. Yu L, Lu M, Jia D, Ma J, Ben-Jacob E, Levine H, et al. Modeling the Genetic Regulation of Cancer Metabolism: Interplay between Glycolysis and Oxidative Phosphorylation. Cancer Res. 2017;77(7):1564–74.

23. Sancho P, Burgos-Ramos E, Tavera A, Bou Kheir T, Jagust P, Schoenhals M, et al. MYC/PGC-1α Balance Determines the Metabolic Phenotype and Plasticity of Pancreatic Cancer Stem Cells. Cell Metab. 2015;22(4):590–605.

24. Jia D, Paudel BB, Hayford CE, Hardeman KN, Levine H, Onuchic JN, et al. Drug-Tolerant Idling Melanoma Cells Exhibit Theory-Predicted Metabolic Low-Low Phenotype. Frontiers Oncol. 2020;10:1426.

25. LeBleu VS, O'Connell JT, Herrera KNG, Wikman H, Pantel K, Haigis MC, et al. PGC-1α mediates mitochondrial biogenesis and oxidative phosphorylation in cancer cells to promote metastasis. Nat Cell Biol. 2014;16(10):992–1003.

26. Dupuy F, Tabariès S, Andrzejewski S, Dong Z, Blagih J, Annis MG, et al. PDK1-Dependent Metabolic Reprogramming Dictates Metastatic Potential in Breast Cancer. Cell Metab. 2015;22(4):577–89.

27. Jia D, Park JH, Kaur H, Jung KH, Yang S, Tripathi S, et al. Towards decoding the coupled decision-making of metabolism and epithelial-to-mesenchymal transition in cancer. Brit J Cancer. 2021;1–10.

28. Georgakopoulos-Soares I, Chartoumpekis DV, Kyriazopoulou V, Zaravinos A. EMT Factors and Metabolic Pathways in Cancer. Frontiers Oncol. 2020;10:499.

29. Fedele M, Sgarra R, Battista S, Cerchia L, Manfioletti G. The Epithelial–Mesenchymal Transition at the Crossroads between Metabolism and Tumor Progression. Int J Mol Sci. 2022;23(2):800.

30. Burger GA, Danen EHJ, Beltman JB. Deciphering Epithelial–Mesenchymal Transition Regulatory Networks in Cancer through Computational Approaches. Frontiers Oncol. 2017;7:162.

31. Hu Y, Xu W, Zeng H, He Z, Lu X, Zuo D, et al. OXPHOS-dependent metabolic reprogramming prompts metastatic potential of breast cancer cells under osteogenic differentiation. Brit J Cancer. 2020;123(11):1644–55.

32. Sung J-Y, Cheong J-H. Pan-Cancer Analysis Reveals Distinct Metabolic Reprogramming in Different Epithelial–Mesenchymal Transition Activity States. Cancers. 2021;13(8):1778.

33. Choudhary KS, Rohatgi N, Halldorsson S, Briem E, Gudjonsson T, Gudmundsson S, et al. EGFR Signal-Network Reconstruction Demonstrates Metabolic Crosstalk in EMT. Plos Comput Biol. 2016;12(6):e1004924.

34. Feng S, Zhang L, Liu X, Li G, Zhang B, Wang Z, et al. Low levels of AMPK promote epithelial-mesenchymal transition in lung cancer primarily through HDAC4- and HDAC5-mediated metabolic reprogramming. J Cell Mol Med. 2020;24(14):7789–801.

35. Kang X, Wang J, Li C. Exposing the Underlying Relationship of Cancer Metastasis to Metabolism and Epithelial-Mesenchymal Transitions. Iscience. 2019;21:754–72.

36. Bocci F, Tripathi SC, Mercedes SAV, George JT, Casabar JP, Wong PK, et al. NRF2 activates a partial epithelial-mesenchymal transition and is maximally present in a hybrid epithelial/mesenchymal phenotype. Integr Biol. 2019;11(6):251–63.

37. Luo M, Shang L, Brooks MD, Jiagge E, Zhu Y, Buschhaus JM, et al. Targeting Breast Cancer Stem Cell State Equilibrium through Modulation of Redox Signaling. Cell Metab. 2018;28(1):69-86.e6.

38. Colacino JA, Azizi E, Brooks MD, Harouaka R, Fouladdel S, McDermott SP, et al. Heterogeneity of Human Breast Stem and Progenitor Cells as Revealed by Transcriptional Profiling. Stem Cell Rep. 2018;10(5):1596–609.

39. Jia D, Li X, Bocci F, Tripathi S, Deng Y, Jolly MK, et al. Quantifying Cancer Epithelial-Mesenchymal Plasticity and its Association with Stemness and Immune Response. J Clin Medicine. 2019;8(5):725.

40. Jolly MK, Tripathi SC, Jia D, Mooney SM, Celiktas M, Hanash SM, et al. Stability of the hybrid epithelial/mesenchymal phenotype. Oncotarget. 2016;7(19):27067–84.

41. Farris JC, Pifer PM, Zheng L, Gottlieb E, Denvir J, Frisch SM. Grainyhead-like 2 Reverses the Metabolic Changes Induced by the Oncogenic Epithelial–Mesenchymal Transition: Effects on Anoikis. Mol Cancer Res. 2016;14(6):528–38.

42. Kovac S, Angelova PR, Holmström KM, Zhang Y, Dinkova-Kostova AT, Abramov AY. Nrf2 regulates ROS production by mitochondria and NADPH oxidase. Biochimica Et Biophysica Acta Bba - Gen Subj. 2015;1850(4):794–801.

43. He F, Ru X, Wen T. NRF2, a Transcription Factor for Stress Response and Beyond. Int J Mol Sci. 2020;21(13):4777.

44. Li N, Muthusamy S, Liang R, Sarojini H, Wang E. Increased expression of miR-34a and miR-93 in rat liver during aging, and their impact on the expression of Mgst1 and Sirt1. Mech Ageing Dev. 2011;132(3):75–85.

45. Bai X-Y, Ma Y, Ding R, Fu B, Shi S, Chen X-M. miR-335 and miR-34a Promote Renal Senescence by Suppressing Mitochondrial Antioxidative Enzymes. J Am Soc Nephrol. 2011;22(7):1252–61.

46. Navarro F, Lieberman J. miR-34 and p53: New Insights into a Complex Functional Relationship. Plos One. 2015;10(7):e0132767.

47. Italiano D, Lena AM, Melino G, Candi E. Identification of NCF2/p67phox as a novel p53 target gene. Cell Cycle. 2012;11(24):4589–96.

48. Chou H-L, Fong Y, Wei C-K, Tsai E-M, Chen JY-F, Chang W-T, et al. A Quinone-Containing Compound Enhances Camptothecin-Induced Apoptosis of Lung Cancer Through Modulating Endogenous ROS and ERK Signaling. Arch Immunol Ther Ex. 2017;65(3):241–52.

49. Serocki M, Bartoszewska S, Janaszak-Jasiecka A, Ochocka RJ, Collawn JF, Bartoszewski R. miRNAs regulate the HIF switch during hypoxia: a novel therapeutic target. Angiogenesis. 2018;21(2):183–202.

50. Shang Y, Chen H, Ye J, Wei X, Liu S, Wang R. HIF-1α/Ascl2/miR-200b regulatory feedback circuit modulated the epithelial-mesenchymal transition (EMT) in colorectal cancer cells. Exp Cell Res. 2017;360(2):243–56.

51. Byun Y, Choi Y-C, Jeong Y, Lee G, Yoon S, Jeong Y, et al. MiR-200c downregulates HIF-1α and inhibits migration of lung cancer cells. Cell Mol Biol Lett. 2019;24(1):28.

52. Xu X, Tan X, Tampe B, Sanchez E, Zeisberg M, Zeisberg EM. Snail Is a Direct Target of Hypoxia-inducible Factor 1α (HIF1α) in Hypoxia-induced Endothelial to Mesenchymal Transition of Human Coronary Endothelial Cells*. J Biol Chem. 2015;290(27):16653–64.

53. Chou C-C, Lee K-H, Lai I-L, Wang D, Mo X, Kulp SK, et al. AMPK Reverses the Mesenchymal Phenotype of Cancer Cells by Targeting the Akt–MDM2–Foxo3a Signaling Axis. Cancer Res. 2014;74(17):4783–95.

54. Ohshima J, Wang Q, Fitzsimonds ZR, Miller DP, Sztukowska MN, Jung Y-J, et al. Streptococcus gordonii programs epithelial cells to resist ZEB2 induction by Porphyromonas gingivalis. Proc National Acad Sci. 2019;116(17):201900101.

55. Huang W, Cao J, Liu X, Meng F, Li M, Chen B, et al. AMPK Plays a Dual Role in Regulation of CREB/BDNF Pathway in Mouse Primary Hippocampal Cells. J Mol Neurosci. 2015;56(4):782–8.

56. Jin H, Xue L, Mo L, Zhang D, Guo X, Xu J, et al. Downregulation of miR-200c stabilizes XIAP mRNA and contributes to invasion and lung metastasis of bladder cancer. Cell Adhes Migr. 2019;13(1):236–48.

57. Janin M, Esteller M. Oncometabolite Accumulation and Epithelial-to-Mesenchymal Transition: The Turn of Fumarate. Cell Metab. 2016;24(4):529–30.

58. Zhang Q, Zheng S, Wang S, Wang W, Xing H, Xu S. Chlorpyrifos induced oxidative stress to promote apoptosis and autophagy through the regulation of miR-19a-AMPK axis in common carp. Fish Shellfish Immun. 2019;93:1093–9.

59. Radisky DC, Levy DD, Littlepage LE, Liu H, Nelson CM, Fata JE, et al. Rac1b and reactive oxygen species mediate MMP-3-induced EMT and genomic instability. Nature. 2005;436(7047):123–7.

60. Babaei G, Raei N, milani AT, Aziz SG-G, Pourjabbar N, Geravand F. The emerging role of miR-200 family in metastasis: focus on EMT, CSCs, angiogenesis, and anoikis. Mol Biol Rep. 2021;48(10):6935–47.